The Double Helix Is Dehydrated: Evidence from the Hydrolysis of Acridinium Ester-Labeled Probes

Michael Becker,* Vicente Lerum, Steve Dickson, Norman C. Nelson, and Eiji Matsuda

Gen-Probe Incorporated, 10210 Genetic Center Drive, San Diego, California 92121

Received November 30, 1998; Revised Manuscript Received February 2, 1999

ABSTRACT: A highly chemiluminescent reporter molecule, acridinium ester (AE), was tethered to single-stranded oligonucleotide probes and hybridized to complementary as well as mismatched target sequences. When tethered to single-stranded probes, AE was readily hydrolyzed by water or hydroxide ion. In contrast, when hybridized to a complementary target, hydrolysis of the AE probe was markedly inhibited. Mismatches near AE eliminated the ability of the double helix to strongly inhibit AE hydrolysis. To establish the molecular basis for these remarkable hydrolysis properties of AE-labeled probes, the binding and hydrolysis mechanisms of AE-labeled probes were examined. When tethered to single- or double-stranded nucleic acids, hydrolysis of AE was found to proceed by generalized base catalysis in which a base abstracts a proton from water and the resulting hydroxide ion then hydrolyzes AE. Analysis of the hydrolysis rates of AE bound to DNA revealed that AE binds the minor groove of DNA and that its hydrolysis is inhibited by low water activity within the minor groove of the helix. Depending upon the sequence of the DNA, the water activity of the minor groove was estimated to be at least 2−4-fold lower than bulk solution. Hydrolysis measurements of AE tethered to RNA as well as RNA/DNA hybrids argued that the grooves of these double helices are also dehydrated relative to bulk solution. Remarkably, mismatched bases, regardless of their structure or sequence context, enhanced hydrolysis of AE by inducing hydration of the double helix that spread approximately five base pairs on either side of the mismatch.

Acridinium ester (AE)[1] is a highly chemiluminescent label used in a variety of diagnostic assays (reviewed in ref *1*). In nucleic acid probe-based assays, AE is attached to single-stranded probes by an abasic linker-arm chemistry that adds one ethylene phosphate group to the backbone of the probe (*2*). The ethylene phosphate group bulges out from the double helix upon hybridization to target sequence, resulting in minimal destabilization of the helix (*2*, *3*). When tethered to nucleic acids in this fashion, AE exhibits remarkable hydrolysis properties that are important for its use in nucleic acid-based diagnostic assays (reviewed in ref *1*). Alkaline solutions readily catalyze the hydrolysis of the ester bond of AE, rendering AE nonchemiluminescent. When AE is tethered to a single-stranded probe, hydrolysis is rapid. In contrast, when an AE-labeled probe is hybridized to a perfectly complementary target, hydrolysis of AE is markedly inhibited. Remarkably, the presence of a single mismatch immediately adjacent to the site of AE attachment strongly inhibits the ability of the double helix to protect AE from hydrolysis (*3*). Here we determine the molecular basis for the differential hydrolysis properties of AE-labeled probes.

MATERIALS AND METHODS

Oligonucleotides. DNA, RNA, and AE-labeled oligonucleotides were prepared as previously described (*3*). The hydrolysis results summarized in Tables 3−5 were obtained by hybridizing the AE-labeled probe 5′-CCGCTGAAGG-C*CGCTTTTCGAACTAAGA-3′, where the asterisk denotes the site of attachment of AE, to the following target sequences: 3′-GGCGACTTCCGGCGAAAAGCTTGATTCT-5′ (hybrid), 3′-GGCGACTTCCAGCGAAAAGCTTGAT-TCT-5′ (1 mismatch), and 3′-GGCGACTTCCATC-GAAAAGCTTGATTCT-5′ (2 mismatches). The hydrolysis and adduct formation measurements summarized in Table 2 were obtained by hybridizing an AE-labeled probe, 5′-CCGGPy$_{10}$*Py$_{10}$GGCC-3′ or 5′-GGCCPu$_{10}$*Pu$_{10}$CCGG-3′, where the asterisk denotes the site of AE attachment and Py denotes a pyrimidine (cytosine, 5-methylcytosine, thymine, or uracil) and Pu denotes a purine (adenine, guanine, or inosine), to its respective complementary target 3′-GGCCPu$_{20}$-CCGG-5′ or 3′-CCGGPy$_{20}$GGCC-5′. The resultant hybrids are denoted in an abbreviated form. Thus hybridization of 5′-GGCCA$_{10}$*A$_{10}$CCGG-3′ to 3′-CCGGT$_{20}$GGCC-5′ yielded the hybrid dA$_{20}$dT$_{20}$. To estimate the binding site size of AE (Figure 1), AE-labeled probes were constructed from the sequence 5′-CCGG(C)$_N$ T$_5$(C)$_M$*(C)$_M$T$_5$(C)$_N$GGCC-3′ where the following combinations of N and M were used in each probe($N = 0$, $M = 6$; $N = 2$, $M = 4$; $N = 4$, $M = 2$; and $N = 5$, $M = 1$). Each probe was then hybridized to a complementary sequence lacking a linker arm and AE. For triple-strand experiments an AE-labeled probe, d(CT), 5′-ATTG-AAACGGTCTTCTCCCTC*TCTCTCTTCCGTTTACAAG-3′, was hybridized to d(GA), 5′-CTTGTAAACGGAAGAGA-GAGAGGGAGAAGACCGTTTCAAT-3′, and d(GA)$_{TR}$, 5′-GGAAGAGAGAGAGAGGGAGAAGA-3′. To compare the hydrolysis properties of a DNA helix containing a water spine

* To whom correspondence should be addressed: Tel 619 410 8832; Fax 1 619 410 8871.

[1] Abbreviations: AE, acridinium ester; nIm, 4-nitroimidazole; SO_3, sodium sulfite.

10.1021/bi9828066 CCC: $18.00
Published on Web 04/03/1999

Table 1: Hydrolysis of AE-Labeled Nucleic Acids in the Presence of Netropsin[a]

species	k_{obs}^{-net}(pr)	k_{obs}^{-net}(hy)	k_{obs}^{+net}(pr)	k_{obs}^{+net}(hy)	k_{obs}^{+net}(hy)/k_{obs}^{-net}(hy)
dU	2.42×10^{-3}	na	1.58×10^{-3}	na	na
dAdT*	1.89×10^{-3}	1.83×10^{-4}	1.8×10^{-3}	9.71×10^{-4}	5.31
dA*dU	nd	2.24×10^{-4}	nd	7.65×10^{-4}	3.42
dI*dC	1.39×10^{-3}	4.28×10^{-4}	1.08×10^{-3}	5.23×10^{-4}	1.22
dIdC*	2.66×10^{-3}	3.03×10^{-4}	2.73×10^{-3}	4.68×10^{-4}	1.54
dT*rA	1.89×10^{-3}	1.74×10^{-5}	1.8×10^{-3}	2.28×10^{-5}	1.3
dG*dC	1.08×10^{-2}	7.36×10^{-5}	1.13×10^{-3}	7.13×10^{-5}	0.97
d(GA)d(CT)*	1.36×10^{-3}	1.93×10^{-4}	na	na	na
d(GA)d(CT)*d(GA)$_{TR}$	1.36×10^{-3}	8.37×10^{-5}	na	na	na
r(GA)d(CT)*	1.36×10^{-3}	4.6×10^{-5}	na	na	na

[a] Observed rate constants (seconds^{-1}) for the hydrolysis of various AE-labeled probes [k_{obs}(pr)]) and corresponding hybrids [k_{obs}(hy)] in the absence (−net) or presence (+net) of netropsin. na, not applicable. nd, experiments not done. The AE-labeled probe is denoted by an asterisk.

to the corresponding RNA helix lacking the spine, an AE-labeled DNA probe, 5′-CCGGA$_{10}$T$_2$*T$_5$GGCC-3′, or an AE-labeled RNA probe, 5′-CCGGA$_{10}$U$_2$*U$_5$GGCC-3′, was hybridized to a complementary DNA or RNA target.

Hydrolysis and Adduct Formation Measurements. Double-stranded hybrids were formed by incubating an AE-labeled probe (0.25×10^{-12} mol) with a target sequence (25×10^{-12} mol) in 30 μL of hybridization buffer [125 mM LiOH, 95 mM succinic acid, 8.5% lithium lauryl sulfate (w/v), 1.5 mM EDTA, and 1.5 mM EGTA, pH 5.1] for 30 min at 60 °C (dI$_{20}$dC$_{20}$* at 45 °C). Hydrolysis was in 600 mM boric acid, 182 mM sodium hydroxide (pH 8.5), and 1% Triton X-100 (hydrolysis buffer). Detection of AE chemiluminescence was as previously described (*3*). Adduct formation rates were measured by placing 10 μL of an AE-labeled probe or hybrid into a 12 × 75 mm polycarbonate test tube and adding 250 μL of a sodium sulfite solution (0.02−10 mM in 60 mM Na_2PO_4, pH 8) to initiate adduct formation.

Netropsin Experiments. Netropsin (Boehringer Mannheim) was dissolved in hydrolysis buffer and its effect on the hydrolysis rate of AE was examined at 35 °C.

Triple Strand Experiments. A double helix was first prepared by hybridizing an AE-labeled d(CT) probe to a complementary d(GA) target for 30 min at 60 °C in hybridization buffer (see above) containing 0.1 mM spermine hydrochloride (Sigma) and 20 mM $MgCl_2$. The third strand, d(GA), was then added and hybridization continued at 60 °C for an additional 20 min followed by incubation at 35 °C for 45 min. The effect of triple-strand formation on the hydrolysis rate of AE was examined at 35 °C.

RESULTS

Binding of AE to DNA. Small planar molecules such as AE are known to bind the double helix by intercalating between adjacent base pairs or by binding to one of the grooves of the helix. In either binding mode, the linker that tethers AE to the helix backbone must deliver AE through the major or the minor groove of DNA. To identify which groove the AE-linker arm resides in, ligands known to bind either the major or the minor groove of DNA were examined for their ability to disrupt AE binding. Since hybridization of an AE-labeled probe to a complementary target protects AE from hydrolysis, agents that disrupt the binding of AE to the duplex enhance the hydrolysis of AE.

To determine whether AE resides in the minor groove of DNA, the effect of netropsin, a known minor-groove-binding drug (reviewed in refs *4* and *5*), on AE hydrolysis rates was examined. AE was first tethered to dAdT, a high-affinity binding sequence for netropsin, and the hydrolysis of AE was examined over a range of netropsin concentrations. The hydrolysis of AE was accelerated by increasing concentrations of netropsin and hydrolysis remained pseudo-first-order up to a concentration of 100 μM netropsin (*6*). Higher concentrations of netropsin interfered with the chemiluminescence of AE and thus were not examined (*6*). Thus, a concentration of 100 μM netropsin was used for all subsequent measurements.

Rate constants for the hydrolysis of AE by hydroxide ion in the absence or presence of 100 μM netropsin are summarized in Table 1. AE was tethered to five different single-stranded probes (dT$_{20}$, dU$_{20}$, dC$_{20}$, dG$_{20}$, and dI$_{20}$) and five double-stranded hybrids (dA$_{20}$dT$_{20}$, dA$_{20}$dU$_{20}$, dI$_{20}$dC$_{20}$, dT$_{20}$rA$_{20}$, and dG$_{20}$dC$_{20}$). In the absence of netropsin all single-stranded probes hydrolyzed at similar rates except dG, which aggregated (*6*) and thus artificially protected AE from hydrolysis. Consistent with its failure to bind single-stranded DNA, netropsin did not significantly alter the hydrolysis rates of AE tethered to these probes. In contrast, when netropsin was added to each hybrid, the hydrolysis rate of AE was increased for all duplexes except dC$_{20}$dG$_{20}$, which does not bind netropsin. There was a strong correlation between the ability of netropsin to increase the hydrolysis of AE and the known binding affinity of netropsin for these sequences. From circular dichroism measurements (*7*) the affinity of netropsin for these sequences followed the order dAdT > dAdU > dIdC > rAdT > dGdC, which was the same order observed for the relative increase in the hydrolysis rate of AE induced by the binding of netropsin to these duplexes. When netropsin bound to the strongest binding duplex, dA$_{20}$dT$_{20}$, the hydrolysis rate of AE was similar to its hydrolysis rate when tethered to dT$_{20}$, consistent with the displacement of AE from the minor groove by netropsin.

To examine the effect of a major-groove-binding ligand on the hydrolysis of AE, the effect of triple helix formation on the hydrolysis of AE was investigated. Previous measurements showed that d(GA) binds to the major groove of d(GA)d(CT) to form a triple helix (*8*). If tethered AE binds the major groove of DNA, then the third strand of the triple helix would be expected to displace AE, thereby accelerating its hydrolysis. As summarized in Table 1, the binding of d(GA) to d(GA)d(CT) to form a triple helix did not increase the hydrolysis of AE but rather decreased the hydrolysis rate 2.3-fold. The hydrolysis rate of AE did not change when the concentration of d(GA) was increased 3-fold (*6*), and

Table 2: Hydrolysis and Adduct Formation Rates of AE-Labeled Probes[a]

species	k_{obs}(pr)	k_{obs}(hy)	k_{obs}(pr)/k_{obs}(hy)	$k_{obs}^{SO_3}$(pr)	$k_{obs}^{SO_3}$(hy)	$k_{obs}^{SO_3}$(pr)/$k_{obs}^{SO_3}$(hy)
dG_{20}·d(5MeC)$_{20}$*	1.23×10^{-3}	4.70×10^{-5}	26.4	nd	nd	nd
dI_{20}·d(5MeC)$_{20}$*	1.23×10^{-3}	3.32×10^{-4}	3.7	nd	nd	nd
dG_{20}·dC_{20}*	1.34×10^{-3}	3.44×10^{-5}	39.8	0.315	8.57×10^{-4}	372
dI_{20}·dC_{20}*	1.34×10^{-3}	3.03×10^{-4}	4.4	0.301	0.33	0.9
dG_{20}*·dC_{20}	3.32×10^{-4}	7.36×10^{-5}	nd	nd	nd	nd
dI_{20}*·dC_{20}	2.57×10^{-3}	4.28×10^{-4}	6.1	nd	nd	nd
dA_{20}*·dT_{20}	1.89×10^{-3}	2.58×10^{-4}	7.4	nd	nd	nd
dA_{20}*·dU_{20}	1.89×10^{-3}	2.24×10^{-4}	8.5	nd	nd	nd
dA_{20}·dT_{20}*	1.89×10^{-3}	1.83×10^{-4}	10.5	0.693	1.03×10^{-2}	67
dA_{20}·dU_{20}*	1.48×10^{-3}	1.83×10^{-4}	8.3	0.385	2.17×10^{-3}	176
rG_{20}·dC_{20}*	1.34×10^{-3}	2.75×10^{-4}	4.8	0.315	6.86×10^{-2}	4.7
rA_{20}·dT_{20}*	1.89×10^{-3}	1.74×10^{-5}	109	0.693	4.91×10^{-4}	1412
$dA_{10}T_2$*T_5·dA_7dT_{10}	4.62×10^{-3}	1.12×10^{-3}	4.1	nd	nd	nd
$rA_{10}U_2$*U_5·rA_7rU_{10}	5.78×10^{-3}	2.65×10^{-4}	21.8	nd	nd	nd

[a] Observed rate constants (seconds^{-1}) for the hydrolysis of various AE-labeled probes [k_{obs}(pr)], and corresponding hybrids [k_{obs}(hy)], as well as the observed rate constants for the formation of a sulfite adduct by each probe [$k_{obs}^{SO_3}$(pr)] and corresponding hybrid [$k_{obs}^{SO_3}$(hy)]. Hydrolysis was in borate buffer (pH 8.5) at 35 °C. Sulfite adduct formation rates were in 2.0 mM sodium sulfite at room temperature. The average standard deviation for hybrolysis and adduct formation rates was 1 SD = ±8%. nd, experiments not done.

gel electrophoresis confirmed the formation of the triple strand in the hydrolysis buffer (*6*). Thus the binding of d(GA) to the major groove did not displace AE and enhance its hydrolysis.

We have previously observed that RNA duplexes of mixed sequence protect AE from hydrolysis more than corresponding DNA duplexes (results not shown). Since triple strands can adopt A-like conformations, the observed decrease in AE hydrolysis could be the result of AE binding to the minor groove of the triplex, which adopts an A-like conformation and thus protects against the hydrolysis of AE. To test this hypothesis we examined the hydrolysis of AE tethered to an RNA/DNA hybrid of the same sequence, r(GA)d(CT), which is expected to adopt an A-like conformation. As summarized in Table 1, this duplex, like the triple strand, protected AE from hydrolysis. Thus the small increase in protection against AE hydrolysis observed when AE is tethered to the triple helix is consistent with the binding of AE to the minor groove of the triplex which adopts an A-like conformation.

A third set of experiments to probe the binding of AE to DNA examined the effect of major- or minor-groove substituents on the hydrolysis of AE. To examine the effect of a major-groove substituent on the hydrolysis of AE, AE was tethered to dG_{20}d(5-MeC)$_{20}$ or $dG_{20}dC_{20}$, dI_{20}d(5-MeC)$_{20}$ or $dI_{20}dC_{20}$, and $dA_{20}dT_{20}$ or $dA_{20}dU_{20}$. Each pair of helixes differs only in whether a methyl group is present in the major groove [d(5-MeC, dT] or not (dC, dU). As summarized in Table 2, the presence of a methyl group in the major groove of each DNA helix altered AE hydrolysis rates only 1.4-fold.

To examine the effect of a minor-groove substituent on the hydrolysis rate of AE, AE was tethered to dG_{20}d(5-MeC)$_{20}$ or dI_{20}d(5-MeC)$_{20}$ and $dG_{20}dC_{20}$ or $dI_{20}dC_{20}$. Each pair of helixes only differ in whether a 2-amino group resides in the minor groove (dG) or not (dI). As summarized in Table 2, the presence of a 2-amino group in the minor groove of each helix markedly decreased (7−9-fold) the hydrolysis of AE.

Taken together, the effect of netropsin, triple-strand formation, and groove substituents on the hydrolysis rates of AE argue that tethered AE binds to the minor groove of DNA.

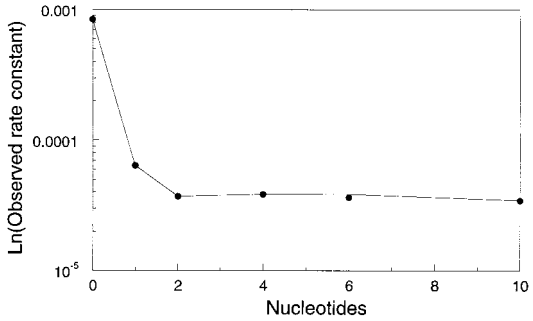

FIGURE 1: Estimation of the binding site size of AE tethered to a double helix. The logarithm of the rate constant for the hydrolysis of AE is plotted against the number of nucleotides that separate a bound netropsin molecule from the site at which AE is inserted into the phosphate backbone.

To estimate the binding site size of AE we exploited the ability of netropsin to displace AE from the minor groove of DNA. Within a $dG_{22}dC_{22}$ helix two netropsin binding sites (dA_5dT_5), one on each side of a tethered AE molecule, were inserted at varying distances from the point of attachment of AE. The effect of adding 100 μM netropsin on the hydrolysis of the tethered AE was then determined for each helix. To estimate the binding site size of AE, the minimum distance at which netropsin molecules interfered with AE hydrolysis was determined. As summarized in Figure 1, the hydrolysis rate of AE did not change when both netropsin molecules were moved to within two bases of the AE attachment site. When this distance was less than two bases the hydrolysis rate of AE was markedly enhanced. We conclude, therefore, that AE covers two bases on one or both sides of its insertion into the DNA backbone.

Mechanism of AE Hydrolysis. To understand how the double helix protects AE from hydrolysis, we first examined the mechanism whereby hydroxide ion hydrolyzes AE. Typically, AE-labeled probes are hydrolyzed in alkaline borate solutions (*1*), where hydrolysis of AE is weakly dependent upon borate and strongly dependent upon hydroxide concentration (results not shown). To examine the hydrolysis of AE by hydroxide ion alone, various AE-labeled species were hydrolyzed over a range of borate (10−90 mM) and hydroxide ion concentrations (pH 8−9.8) and the results were extrapolated to zero borate concentration. Four AE

Table 3: Hydrolysis of AE-Labeled Nucleic Acids[a]

AE species	$k_{obs}^{H_2O}$ (s^{-1})	k_{obs}^{OH} (s^{-1})	relative rates (60 °C) $k_{obs}^{H_2O}$ (s^{-1})	relative rates (60 °C) k_{obs}^{OH} (s^{-1})
probe	$(2.3 \pm 1.1) \times 10^{-2}$	4567 ± 666	1.00	1.00
2 mismatches	$(3.4 \pm 0.8) \times 10^{-3}$	897 ± 47	0.15	0.20
1 mismatch	$(1.6 \pm 0.6) \times 10^{-3}$	370 ± 20	0.07	0.08
hybrid	$(7.0 \pm 1.5) \times 10^{-4}$	203 ± 5	0.03	0.04

AE species	$k_{obs}^{H_2O}$ (s−1)	k_{obs}^{OH} (s^{-1})	relative rates (42 °C) $k_{obs}^{H_2O}$ (s^{-1})	relative rates (42 °C) k_{obs}^{OH} (s^{-1})
probe	$(1.9 \pm 0.7) \times 10^{-3}$	524 ± 41	1.00	1.00
2 mismatches	$(2.2 \pm 0.4) \times 10^{-4}$	52 ± 1	0.12	0.10
1 mismatch	$(1.2 \pm 0.5) \times 10^{-4}$	26 ± 3	0.06	0.05
hybrid	nd	14.7 ± 0.04	nd	0.03

AE species	k_{obs}^{nIm} (s^{-1})	$k_{obs}^{OH(n\ Im)}$ (s^{-1})	relative rates (42 °C) k_{obs}^{nIm} (s^{-1})	relative rates (42 °C) $k_{obs}^{OH(nIm)}$ (s^{-1})
probe	0.87 ± 0.05	77 ± 19	1.00	1.00
2 mismatches	$(3.24 \pm 0.19) \times 10^{-2}$	8.7 ± 0.6	0.04	0.11
1 mismatch	$(1.61 \pm 0.06) \times 10^{-2}$	4.8 ± 0.2	0.02	0.06
hybrid	$(1.51 \pm 0.07) \times 10^{-2}$	1.6 ± 0.3	0.02	0.02

[a] Obeserved rate constants for the hydrolysis of various AE species by water ($k_{obs}^{H_2O}$), hydroxide ion (k_{obs}^{OH}), nitroimidazole ion (k_{obs}^{nIm}), and hydroxide ion in nitroimidazole buffer ($k_{obs}^{OH(nIm)}$) at 42 °C or 60 °C. nd, experiments not done.

species were examined: AE-labeled probe (probe), AE-labeled probe hybridized to a complementary target (hybrid), and the same AE hybrid containing either one (1 mismatch) or two adjacent mismatches (2 mismatches) immediately adjacent to the site of the linker arm used to attach AE. A plot of the observed hydrolysis rate constants versus the concentration of hydroxide ion was linear over the pH range examined (results not shown) and the slope and intercept for each species yielded estimates of the rate constants for the pH-dependent hydrolysis of AE by hydroxide ion (k_{obs}^{OH}) and the pH-independent hydrolysis by water ($k_{obs}^{H_2O}$), respectively (*9*). The results observed at two different temperatures, 42 and 60 °C, are summarized in Table 3.

Hydrolysis of each AE species by water or hydroxide ion alone followed the order probe > 2 mismatches > 1 mismatch > hybrid. Similar results were observed previously in alkaline borate buffer (*3*). Remarkably, although the rate constants observed for hydroxide ion were 200 000-fold higher than the corresponding rate constants for water, the relative rate constants for each AE species, normalized to AE probe, were essentially identical for water and hydroxide ion. Two important conclusions emerge from these results. First, because hydrolysis by water is a pH-independent process, the double helix does not protect AE from hydrolysis by providing an environment of lower pH than bulk solution. Second, the fact that the relative rate constants for the hydrolysis of AE by water and hydroxide ion varied identically from one AE species to the next argues strongly that water and hydroxide ion hydrolyze AE by mechanisms that proceed through the same rate-limiting step.

The activation energies (E_{act}) required for water or hydroxide ion to hydrolyze a given AE species were calculated from an Arrhenius plot of the temperature dependency of $k_{obs}^{H_2O}$ and k_{obs}^{OH} in Table 3. As summarized in Table 4, the activation energy required for water or hydroxide ion to hydrolyze a given AE species was the same, supporting the conclusion that water and hydroxide ion hydrolyze AE by mechanisms that proceed through the same rate-limiting step.

Table 4: Energy of Activation for AE-Labeled Nucleic Acids

	E_{act} (kcal/mol)	
	H_2O	OH^-
probe	28 ± 11	25 ± 2.6
2 mismatches	31.5 ± 4.9	32.8 ± 0.8
1 mismatch	30 ± 9.7	30.6 ± 2.0
hybrid	nd	30.1 ± 0.3

Table 5: Deuterium Isotope Effects on the Hydrolysis of AE-Labeled Nucleic Acids[a]

AE species	$k_{obs}^{H_2O}$ (s^{-1})	$k_{obs}^{D_2O}$ (s^{-1})	$k_{obs}^{H_2O}/k_{obs}^{D_2O}$
probe	$(1.9 \pm 0.7) \times 10^{-3}$	$(6.8 \pm 2.4) \times 10^{-4}$	2.8 ± 1.0
2 mismatches	$(2.2 \pm 0.4) \times 10^{-4}$	$(2.9 \pm 0.5) \times 10^{-5}$	7.6 ± 1.9
1 mismatch	$(1.2 \pm 0.5) \times 10^{-4}$	$(2.5 \pm 0.1) \times 10^{-5}$	4.8 ± 2.0
hybrid	nd	$(1.2 \pm 1.7) \times 10^{-6}$	nd

AE species	k_{obs}^{OH} (s^{-1})	k_{obs}^{OD} (s^{-1})	$k_{obs}^{OH}/k_{obs}^{OD}$
probe	524 ± 41	393 ± 12	1.3 ± 0.10
2 mismatches	52 ± 1	43 ± 0.2	1.2 ± 0.02
1 mismatch	26 ± 3	13.8 ± 0.07	1.9 ± 0.20
hybrid	14.7 ± 0.04	4.4 ± 0.09	3.3 ± 0.07

AE species	$k_{obs}^{nIm(H_2O)}$ (s^{-1})	$k_{obs}^{nIm(D_2O)}$ (s^{-1})	$k_{obs}^{nIm(H_2O)}/k_{obs}^{nIm(D_2O)}$
probe	0.87 ± 0.05	0.37 ± 0.007	2.3
2 mismatches	$(3.24 \pm 0.2) \times 10^{-2}$	$(5.5 \pm 0.2) \times 10^{-3}$	5.9

AE species	$k_{obs}^{OH(nIm)}$ (s^{-1})	$k_{obs}^{OD(nIm)}$ (s^{-1})	$k_{obs}^{OH(nIm)}/k_{obs}^{OD(nIm)}$
probe	77 ± 19	9.8 ± 1.6	7.7
2 mismatches	8.7 ± 0.6	3.8 ± 0.03	2.3

[a] Observed rate constants at 42 °C for the hydrolysis of various AE species by water ($k_{obs}^{H_2O}$), deuterium oxide ($k_{obs}^{D_2O}$), hydroxide ion (k_{obs}^{OH}), deuterioxide ion (k_{obs}^{OD}), nitroimidazole ion in water ($k_{obs}^{nIm(H_2O)}$), nitroimidazole in deutriumoxide ($k_{obs}^{nIm(D_2O)}$), hydroxide ion in nitroimidazole buffer ($k_{obs}^{OH(nIm)}$) and deuterioxide in nitroimidazole buffer ($k_{obs}^{OD(nIm)}$). nd, experiments not done.

Previous measurements have shown that the hydrolysis of many esters by a water molecule occurs by way of generalized base catalysis in which water acts as a generalized base, abstracting a hydrogen atom from a second water molecule, which then hydrolyzes the ester (*9*). To examine whether water hydrolyzes AE by a similar mechanism, the hydrolysis experiment described above was repeated in D_2O and the rate constants for the hydrolysis of AE by D_2O ($k_{obs}^{D_2O}$) and deuterium oxide ion (k_{obs}^{OD}) determined. Generalized base catalysis of esters by water is 2−4-fold slower in D_2O than in H_2O (*9*). As summarized in Table 5, hydrolysis of each AE species by water was 2.8−7.6-fold slower in D_2O than in H_2O, supporting the conclusion that hydrolysis of AE by water proceeds by general base catalysis.

If hydroxide ion also hydrolyzes AE by generalized base catalysis, then OD^- should hydrolyze AE more slowly than OH^-. In contrast, if hydroxide hydrolyzes AE by direct nucleophilic attack, the hydrolysis of each AE species by OD^- would be expected to be 1.4−2-fold faster than by OH^-

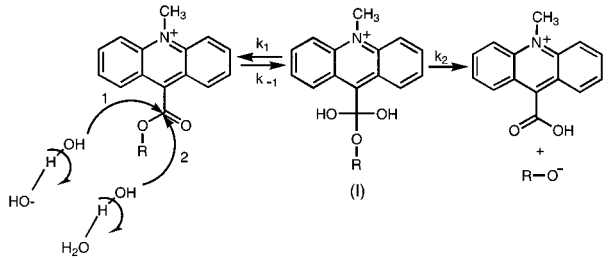

FIGURE 2: Generalized base catalysis of AE by hydroxide ion or water. R represents a substituted phenyl ring that is used to attach AE to a nucleic acid (1). See text for additional details.

(*9*). As summarized in Table 5, hydrolysis of each AE species by OD^- was 1.2−3.3-fold slower than by OH^-. Thus, like water, hydroxide ion also appears to hydrolyze each AE species by generalized base catalysis.

In Figure 2 the mechanism of generalized base catalysis of AE by water or hydroxide is summarized. In both cases a general base (e.g., water or hydroxide ion) abstracts a proton from water that then attacks the carbonyl group of AE. Because generalized base catalysis can be mediated by any base, we also examined the hydrolysis of each AE species by 4-nitroimidazole, a base whose structure is unrelated to water or hydroxide ion. Hydrolysis was examined at 42 °C in H_2O over a range of nitroimidazole concentrations (3−15 mM) at constant pH (9.5). A plot of the observed rate constants versus nitroimidazole concentration was linear (results not shown), and the intercept and slope yielded estimates of the rate constants for the hydrolysis of AE by hydroxide ion plus water ($k_{obs}^{OH(nIm)} + k_{obs}^{H_2O(nIm)}$) and nitroimidazole ion ($k_{obs}^{(nIm)}$), respectively (*9*). Because hydroxide ion hydrolyzes AE much faster than water (Table 3), the quantity ($k_{obs}^{OH(nIm)} + k_{obs}^{H_2O(nIm)}$) reduces to ($k_{obs}^{OH(nIm)}$). For hydroxide ion, the relative rate constants observed in nitroimidazole buffer for each AE species, normalized to AE probe, were in excellent agreement with the relative rate constants measured for hydroxide ion in borate buffer (Table 3). For hydrolysis by nitroimidazole ion, the relative rate constants for each AE species, normalized to AE probe, were somewhat lower than those observed for water or hydroxide ion. When hydrolysis of two different AE species by nitroimidazole was repeated in D_2O, hydrolysis by hydroxide ion as well as nitroimidazole ion was 2.3−7.7 times slower than in H_2O, as expected if both compounds hydrolyze AE by generalized base catalysis (Table 5). On the basis of our analysis of the hydrolysis of AE by water, hydroxide ion, and nitroimidazole, we conclude that the hydrolysis of AE in aqueous solutions proceeds by way of generalized base catalysis.

Because generalized base catalysis of AE is slower in D_2O than H_2O, formation rather than breakdown of the tetrahedral intermediate (I) is rate-limiting. Experiments examining the hydrolysis of AE derivatives containing substituents on the acridinium and/or phenyl ring support this conclusion (*10*). When formation of I is rate-limiting, the hydrolysis of AE by water can be described by the steady-state rate expression

$$-\left(\frac{\partial[AE]}{\partial t}\right)_{H_2O} = k_1^{H_2O}[AE][H_2O]_g^2 = k_{obs}^{H_2O}[AE] \quad (1)$$

where $[H_2O]_g$ is the concentration of water in the vicinity of AE and

$$k_{obs}^{H_2O} = k_1^{H_2O}[H_2O]_g^2 \quad (2)$$

Because AE binds to the minor groove of DNA, $[H_2O]_g$ is the concentration of water in the minor groove when AE is bound to a DNA duplex. The corresponding steady-state rate expression for the hydrolysis of AE by hydroxide ion is given by

$$-\left(\frac{\partial AE}{\partial t}\right)_{OH} = k_1^{OH}[AE][H_2O]_g[OH]_g \quad (3)$$

where $[OH]_g$ is the concentration of hydroxide ion in the vicinity of AE. From the autoprotolysis of water we can write

$$[OH]_g = \frac{K_w[H_2O]_g}{[H^+]_g} = \frac{[OH]_s[H^+]_s[H_2O]_g}{[H_2O]_s[H^+]_g} \quad (4)$$

where $[H^+]_g$ is the concentration of hydronium ions in the vicinity of AE, K_w is the autoprotolysis constant, $[OH]_s$ is the concentration of hydroxide ion in solution, $[H^+]_s$ is the concentration of hydronium ions in solution, and $[H_2O]_s$ is the concentration of water in solution. Substituting eq 4 into eq 3 yields

$$-\left(\frac{\partial AE}{\partial t}\right) = k_1^{OH}[AE][H_2O]_g^2[OH]_s\frac{[H^+]_s}{[H_2O]_s[H^+]_g} = k_1^{OH}K[AE][H_2O]_g^2[OH]_s$$

$$= k_{obs}^{OH}[AE][OH]_s \quad (5)$$

where $K = [H^+]_s/[H_2O]_s[H^+]_g$ and

$$k_{obs}^{OH} = k_1^{OH}K[H_2O]_g^2 \quad (6)$$

Because, experimentally, k_{obs}^{OH} and $k_{obs}^{H_2O}$ varied identically from one AE species to the next (Table 3), both rate constants contain a common term and this term must vary identically between different AE species. Comparing eqs 2 and 6, the rate constants k_{obs}^{OH} and $k_{obs}^{H_2O}$ contain a common term, $[H_2O]_g^2$, the square of the water concentration in the vicinity of each AE species. Thus if the concentration of water in the vicinity of AE is different for each AE species, then both k_{obs}^{OH} and $k_{obs}^{H_2O}$ will vary identically between different AE species in accord with our experimental results. Alternatively, $[H_2O]_g^2$ may not differ from one AE species to the next. Rather, steric factors that control the rate at which H_2O or hydroxide attack AE (contained in $k_1^{H_2O}$ and k_1^{OH}) may be different for each AE species. For example, since water and hydroxide ion catalyze the hydrolysis of AE by nearly identical mechanisms (Figure 2), steric factors could be identical for both hydrolytic reactions, resulting in identical variations in k_{obs}^{OH} and $k_{obs}^{H_2O}$ from one AE species to the next.

Steric Factors in AE Hydrolysis Rates. To examine the role of steric factors in AE hydrolysis rates, we examined the hydrolysis as well as the binding of AE tethered to single-stranded probes and corresponding double-stranded hybrids constructed from simple repetitive sequences. To measure the binding of tethered AE to these sequences, we utilized a technique based on the differential reactivity of an AE-labeled probe and corresponding double-stranded hybrid with

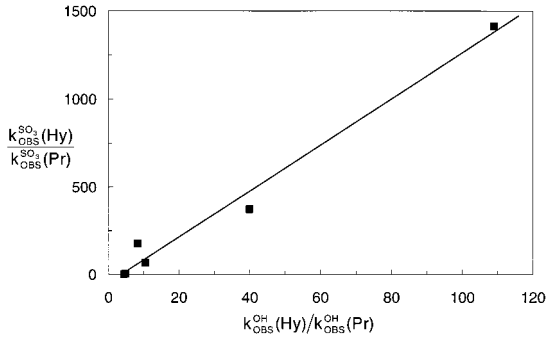

FIGURE 3: Plot of the ability of 6 different double-stranded hybrids to protect AE from adduct formation with sodium sulfite versus the ability of the same hybrids to protect AE from hydrolysis. Adduct formation is expressed as the ratio $k_{obs}^{SO_3}(hy)/k_{obs}^{SO_3}(pr)$, while hydrolysis is expressed as the ratio $k_{obs}^{OH}(hy)/k_{obs}^{OH}(pr)$. See text for details.

sodium sulfite. Sodium sulfite, like many other nucleophiles, reacts reversibly with the C-9 position of AE to form an adduct that inhibits the chemiluminescence of AE (*11*, *12*). When AE is tethered to a single-stranded probe, reaction with sodium sulfite is rapid. In contrast, when an AE-labeled probe is hybridized to a complementary target, reaction with sodium sulfite is much slower (*2*, *12*).

The ability of sodium sulfite to discriminate between an AE-labeled probe and AE-labeled hybrid is not due to the negative charge on sodium sulfite since glycol sulfite, as well as other uncharged compounds, also strongly discriminated between AE-labeled probes and hybrids (*12*). As the size of sodium sulfite was increased from dimethylsulfite to dipropylsulfite, reaction rates with an AE-labeled hybrid or AE-labeled single strand decreased 50−75-fold. Thus duplex formation appears to protect an AE-labeled probe from reaction with sodium sulfite by sterically restricting attack by the bulky sulfite ion.

Because the size of a sulfite ion or a hydroxide ion hydrogen-bonded to a water molecule are similar to one another, and because the C-9 position of AE is located only one carbon bond away from the ester carbonyl that undergoes hydrolysis, steric constraints that restrict sodium sulfite reaction rates are anticipated to be similar to steric constraints that restrict hydrolysis of the ester bond.

In Table 2, rate constants for hydrolysis and sodium sulfite adduct formation are summarized for single-stranded AE-labeled probes constructed from these simple repetitive sequences. All single-stranded probes except dG_{20}, which aggregated and thus artificially protected AE from hydrolysis, hydrolyzed at similar rates or reacted with sodium sulfite at similar rates. In contrast, double-stranded hybrids constructed from these sequences hydrolyzed or reacted with sodium sulfite at very different rates from one another. Because adduct formation is much faster than hydrolysis, we normalized both results by dividing the observed hydrolysis and adduct formation rate constants for each hybrid [$k_{obs}^{OH}(hy)$, $k_{obs}^{SO_3}(hy)$] by the corresponding hydrolysis and adduct formation rate constants for the single-stranded probe ($k_{obs}^{OH}(pr)$, $k_{obs}^{SO_3}(pr)$]. A plot of the ratio $k_{obs}^{SO_3}(hy)/k_{obs}^{SO_3}(pr)$ versus $k_{obs}^{OH}(hy)/k_{obs}^{OH}(pr)$ was linear over a broad range of hydrolysis and adduct formation rate constants (Figure 3). Thus for these simple sequences a good correlation was observed between the ability of a double-stranded hybrid to prevent sodium sulfite from adding to AE and the ability of that hybrid to restrict hydrolysis of AE by a hydroxide ion−water pair. From the slope of the results in Figure 3 we estimate that a double-stranded helix inhibits the reaction of AE with sulfite 13-fold more strongly than it inhibits the hydrolysis of AE by hydroxide ion. Thus if the double helix sterically restricts hydrolysis of AE, steric constraints imposed by the helix on the hydrolysis reaction must be less than those imposed on the sulfite addition reaction.

Although the double helices examined in Table 2 protected AE from hydrolysis as well as from reaction with sulfite ion, the double helix dIdC exhibited anomalous behavior. When tethered to dIdC, AE was hydrolyzed 4−6-fold more slowly than when it was tethered to dI or dC. In contrast, when AE was tethered to dIdC it reacted with sulfite at the same rate as when it was tethered to dC. Control experiments showed that dIdC was a stable duplex under these conditions. Furthermore, the failure of dIdC to protect AE from reaction with sodium sulfite was observed over a broad range of sulfite concentrations (0.02−10 mM) and was also observed with a larger adduct-forming compound, *n*-propylmercaptan. Thus, when bound to dIdC, AE was protected from hydrolysis but not from reaction with bulky adduct-forming compounds. Because steric factors that restrict reaction of AE with sodium sulfite are greater than steric factors that restrict hydrolysis of AE by hydroxide ion, AE tethered to dIdC should be freely accessible to attack by hydroxide ion. Thus we conclude that the ability of dIdC to protect AE from hydrolysis but not sulfite addition was not due to steric factors imposed by the double helix that sterically restrict hydrolysis.

Hydrolysis of AE by Mismatches. Previously we showed that all 12 single-base mismatches accelerated the hydrolysis of AE by alkaline solutions when each mismatch was immediately adjacent to the site at which AE was tethered to the double-stranded helix (*3*). The results presented here (Tables 3−5) argue that mismatches enhance hydrolysis of AE either by inducing hydration of the helix or by enhancing the accessibility of tethered AE to attack by water. To distinguish between these two hypotheses, we examined whether mismatches distal to an AE insertion site could alter adduct formation rates as well as hydrolysis rates of AE. Previous X-ray crystallographic measurements have shown that mismatches only cause small changes in the double helix that are largely localized to the mismatch and the base pair on either side of the mismatch (reviewed in ref *13*). Thus, if mismatches enhance the hydrolysis of AE by enhancing the steric accessibility of AE to attack by water, then the hydrolysis and adduct formation rates of AE should be enhanced only when AE is tethered immediately adjacent to the mismatch or to the base on either side of the mismatch.

To carry out these measurements, the position of AE relative to various single-and double-base mismatches was varied (Figure 4A) and the corresponding hydrolysis and sulfite addition rates were measured. As summarized in Figure 4B, mismatches either weakly inhibited or weakly enhanced reaction of AE with sulfite, and these altered rates were observed only at the mismatched base or at one base on either side of the mismatch. Thus these results argue that the structure and hence the steric accessibility of AE to sulfite addition is altered at the mismatched base and the immediate base on either side, in excellent agreement with X-ray crystallographic measurements.

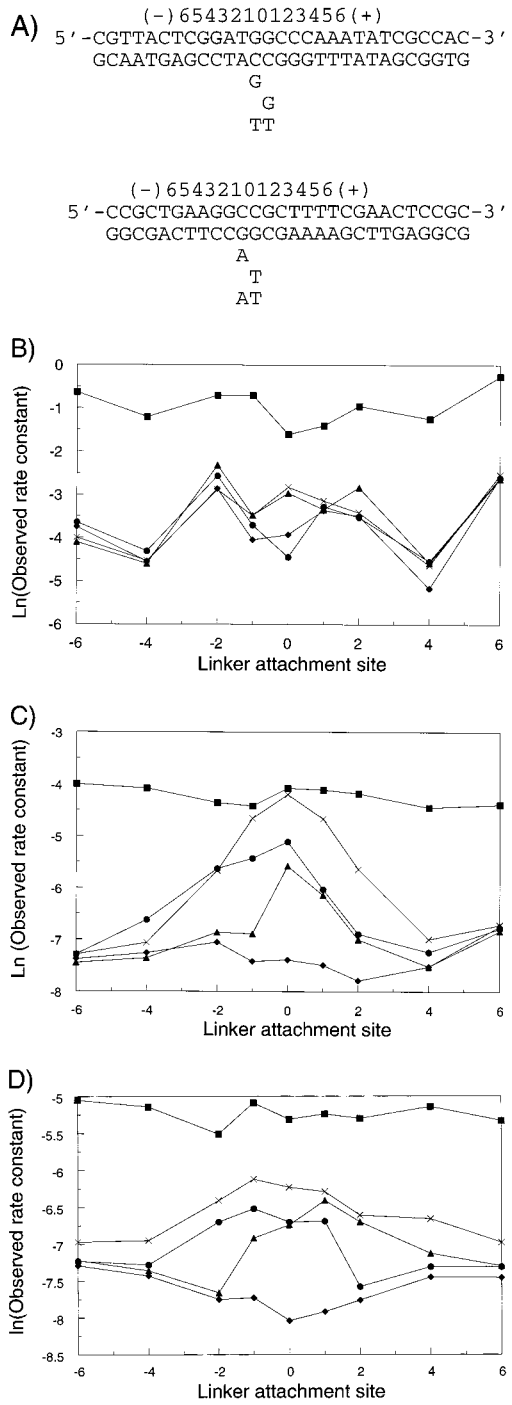

FIGURE 4: Dependence of the logarithm of the rate constant (seconds^{-1}) on the position of the AE attachment site for the reaction of sulfite ion with AE (B) or the hydrolysis of AE (C, D). (A) Sequences used in the analysis. The upper double-stranded sequence was used in panels B and C and the lower sequence was used in panel D. The locations of the single- and double-base mutants in the target strand that were analyzed are shown below each double-stranded sequence. For each sequence the upper strand was the AE-labeled probe and the lower strand was the target. The location of the AE attachment site between adjacent bases is denoted by negative or positive numbers above the sequence. AE was attached to either a single-stranded probe (■), the corresponding matched double-stranded hybrid (◆) or the same hybrid containing a single mismatch between positions 0 and −1 (●), a single mismatch between positions 0 and 1 (▲), or a double mismatch between positions −1 and 1 (×).

In contrast to the sulfite addition results, hydrolysis measurements revealed that the same mismatches [as well as all others examined (*3*; results not shown)] always enhanced the hydrolysis of AE. Furthermore, these mismatches, when located as far away as 4−5 bases on either side of AE, enhanced the hydrolysis rate of AE (Figure 4C). Similar results were observed for a different sequence containing different mismatches (Figure 4D) or when the hydrolyzing species was water rather than hydroxide ion (results not shown). As the number of contiguous mismatched bases increased from 1 to 2 (Figure 4C,D) and then to 3 (results not shown), the distance that the mismatch could be located away from AE and still alter its hydrolysis rate increased. Thus the shapes of the hydrolysis curves in Figure 4C,D are a consequence of the mismatch and not an artifact induced by tethering AE to the backbone of the hybrid. We conclude, therefore, that the steric factors that control the reaction of sodium sulfite with AE tethered to a mismatched hybrid are not the same as those factors that enhance the hydrolysis of AE tethered to the same mismatched hybrids.

Hydrolysis of AE by the Water Spine. To examine the role of water concentration in AE hydrolysis rates, we measured the hydrolysis of AE tethered to the same simple repetitive sequences examined above. Previous X-ray analyses have revealed that narrow minor grooves of DNA, found in AT-rich sequences, are bound by a spine of water (reviewed in ref *14*). IC base pairs, whose minor groove is identical to that of AT base pairs, also bind the water spine (*15*). In contrast, the spine is absent from wide minor grooves found in GC-rich sequences (*16*), A-form DNA (*11*), and RNA (*17*). Because AE binds within the minor groove of DNA, the absence or presence of the spine in the minor groove allowed us to directly assess the role of water in the hydrolysis of AE. Referring to Table 2, we found an excellent correlation between the expected presence or absence of a water spine in these simple sequences and the extent of protection of AE from hydrolysis. Sequences that can bind the spine ($dA_{20}dT_{20}$, $dA_{20}dU_{20}$, $dI_{20}dC_{20}$, and $dI_{20}d5\text{-}MeC_{20}$) did not strongly protect AE from hydrolysis, while sequences that cannot bind the spine ($dG_{20}dC_{20}$, and $dG_{20}d5\text{-}MeC_{20}$) did. The 2-amino group of guanine, which can interfere sterically with the spine (*16*), clearly inhibited hydrolysis of AE since hydrolysis was much slower when AE was tethered to $dG_{20}dC_{20}$ sequences than when it was tethered to $dA_{20}dT_{20}$ or $dI_{20}dC_{20}$ sequences. The mere presence of the 2-amino group was not responsible for preventing hydrolysis of AE tethered to GC base pairs since AE tethered to rGdC, a duplex that should not bind the spine, was readily hydrolyzed. Thus the ability of the 2-amino group to protect AE from hydrolysis appears to be due to the ability of the 2-amino group to disrupt the water spine rather than by other mechanisms.

Although some sequences in DNA such as AAATTT adopt a narrow hydrated minor groove, the corresponding sequence in RNA, AAAUUU, adopts a wide dehydrated groove (*17*). We therefore examined the hydrolysis of AE tethered to two such duplexes, $dA_{10}dT_2{*}dT_5$ and $rA_{10}rU_2{*}rU_5$, where the asterisk denotes the AE attachment site. Previous NMR measurements showed that the AAATTT sequence in the DNA helix binds a water spine while the AAAUUU sequence in the RNA helix does not (*17*). As summarized in Table 2, AE exhibited similar hydrolysis rates when tethered to the DNA and RNA single strands. In contrast, when tethered to the RNA helix AE was hydrolyzed 4−5

times more slowly than when it was tethered to the corresponding DNA helix. Thus the presence of a water spine in the DNA sequence was associated with fast hydrolysis of AE, while the absence of a water spine in the corresponding RNA helix was associated with slow hydrolysis of AE. Taken together, these data and the hydrolysis data of the simple repetitive sequences in Table 2 provide direct support for the conclusion that the hydrolysis rates of AE are proportional to the concentration of water within the local vicinity of AE.

DISCUSSION

The measurements presented here provide a molecular basis for the remarkable ability of double-helical DNA to protect tethered AE from hydrolysis. We first examined how tethered AE binds DNA. Although our measurements did not distinguish whether AE binds in an intercalative or groove-binding mode, they did establish that tethered AE resides in the minor groove of DNA and covers approximately 2 bases on one or both sides of its point of insertion into the DNA backbone. We then demonstrated that the hydrolysis of AE tethered to either a single-stranded probe, a double-stranded duplex, or a double-stranded duplex containing one or two mismatches proceeded by generalized base catalysis in which a base (e.g., water, hydroxide ion, or nitroimidazole) abstracts a proton from a water molecule that then attacks the carbonyl ester of AE. As a result, the rate at which water or hydroxide ion catalyzes the hydrolysis of AE will be dependent on the water concentration in the vicinity of AE as well as the accessibility of the carbonyl ester to attack by a water molecule. Because double-helical DNA was found to protect tethered AE from hydrolysis by water, and because hydrolysis by water is a pH-independent process, the possibility that the minor groove protects AE from hydrolysis by providing a low-pH environment was excluded.

In a second set of experiments, we demonstrated that it was unlikely that the ability of the minor groove of DNA to protect AE from hydrolysis was due to steric factors imposed by the groove that restrict accessibility of the carbonyl ester to attack by a water. This conclusion was based on the reaction of AE with sodium sulfite, whose reversible binding to the C-9 position of AE is sterically restricted when AE is tethered to a double-stranded hybrid. We demonstrated that double helices constructed from simple repetitive sequences protected tethered AE from reaction with sulfite 13 times more strongly than they protected tethered AE from hydrolysis. Thus, if the double helix sterically restricts hydrolysis of AE, steric constraints imposed by the helix on the hydrolysis reaction must be less than those imposed on the sulfite addition reaction. We then demonstrated that dIdC protected AE from hydrolysis but not from reaction with sulfite. Because AE tethered to dIdC is freely accessible to attack by sulfite ion, it should also be freely accessible to attack by hydroxide ion. Thus we concluded that the ability of dIdC to protect AE from hydrolysis but not sulfite addition was not due to steric factors imposed by the double helix that sterically restrict attack by hydroxide ion. Our measurements therefore argued that the slow hydrolysis rate of AE tethered to dIdC was due to the low water activity within the minor groove of dIdC.

To directly assess the role of water concentration in controlling AE hydrolysis rates in other sequences, we examined the hydrolysis of AE tethered to eight different sequences that are known to contain different amounts of water within their minor grooves. These measurements revealed that those sequences that can bind a spine of hydration within their minor groove hydrolyzed AE much more readily than those sequences that cannot bind the spine. Since the spine can bind additional water molecules, we speculate that the spine enhances AE hydrolysis by increasing the concentration of water molecules in the minor groove.

Additional support for the role of water concentration in controlling AE hydrolysis rates came from our analysis of the effects of mismatches on the hydrolysis rates of AE. As previously shown, all single-base mismatches immediately adjacent to AE increased its hydrolysis rate (*3*). By varying the position of AE relative to various mismatches, we were able to show that mismatches located as far away as five bases on either side of AE enhanced its hydrolysis rate. As AE was brought closer to the mismatch, the hydrolysis rate of AE increased steadily, peaked when the mismatch was located at the site of AE insertion, and then fell steadily as AE was moved away from the mismatch. Thus our measurements argued that mismatches induce rehydration of the double helix that spreads for approximately 4−5 bases on either side of the mismatch.

This conclusion is in excellent agreement with previous NMR measurements that examined the effect of a GA mismatch on the hydration of a DNA oligonucleotide duplex (*18*). A single mismatch was shown to enhance hydration of the oligonucleotide and enhanced hydration spread for a distance of 4−5 bases from the mismatch. Because water molecules hydrogen-bond to one another, introduction of a water molecule at the site of a mismatch would be expected to attract other water molecules, spreading hydration from the site of the mismatch. However, owing to thermal disruption of the weak hydrogen bonds between water molecules, the concentration of water molecules should drop steadily as one moves away from the mismatch. The shapes of our AE hydrolysis curves are in excellent agreement with both of these expectations.

Since the hydrolysis curves shown in Figure 4 were also seen for 14 other mismatches (results not shown) and were not significantly affected by the sequence of the mismatch or the sequence context of the flanking sequence (Figure 4D and results not shown), all mismatches appear to induce rehydration of the double helix. Direct evidence for the ability of mismatches to induce hydration of the double helix has been obtained by X-ray crystallographic measurements. For many different mismatches, mispairing between bases exposes hydrogen-bond donor and acceptor groups on the bases that are free to bind water molecules, resulting in enhanced hydration of the helix (reviewed in refs *19* and *20*). Because all mismatches appear to induce hydration of the double helix, repair proteins that recognize mismatches may do so, in part, by their ability to detect patches of water along the grooves of the helix.

In contrast to the hydrolysis curves in Figure 4C, reaction of the same set of AE-labeled molecules with sodium sulfite yielded very different results (Figure 4B). Whereas mismatches always increased hydrolysis rates of AE, mismatches inhibited as well as enhanced reaction of sodium sulfite with AE. Furthermore, when mismatches were located more than 1 base away from AE they did not affect the reaction of

sodium sulfite with AE. Because formation of a double helix protects AE, sterically, from reaction with sodium sulfite, these measurements argued that structural alterations induced by a mismatch are confined to the mismatch and the immediate base pair on either side of the mismatch. This conclusion is in excellent agreement with previous X-ray measurements that showed that mismatches only cause small changes in the double helix that are largely confined to the mismatch and immediate nearest neighbors (*13*).

To estimate the extent of hydration induced in the double helix by mismatches, the hydrolysis rate constants of a perfectly matched duplex can be compared to that of the same duplex containing one or two adjacent mismatches. As shown in Figure 4B, when a single or double mismatch was located one base away from AE (position +1), the rate at which sodium sulfite reacted with the C-9 position of AE was the same for the matched as well as the mismatched duplexes. Thus AE is equally accessible to attack by sodium sulfite in both the matched and mismatched duplexes. Since steric constraints that restrict hydrolysis of AE are no greater than steric constraints that restrict sodium sulfite reaction rates of AE (Figure 3), it is reasonable to assume that AE is equally accessible to attack by a water molecule in both the matched and mismatched duplexes. Differences between the hydrolysis rate constants of matched and mismatched hybrids should therefore be largely due to differences in the concentration of water in the vicinity of AE. From the data in Figure 4C we calculate that the single-mismatched hybrids were hydrolyzed 4-fold faster than the matched hybrid, while the double-mismatched hybrid was hydrolyzed 16-fold faster. Because hydrolysis rate constants for AE are proportional to the square of the concentration of water in the vicinity of AE (eqs 2 and 6), the single and double mismatches are estimated to increase the hydration of the double helix 2- and 4-fold, respectively.

Because the concentration of water in the grooves of a mismatched hybrid will not exceed the concentration of water in bulk solution, the concentration of water in our experiments follows the order bulk solution > mismatched duplex groove > matched duplex groove. Therefore the increase in water concentration induced by a double mismatch (4-fold) is also equal to the minimal difference between the concentration of water in the groove of a matched duplex and the concentration of water in bulk solution. If hydrolysis rates of AE tethered to single- and double-stranded nucleic acids are subject to similar steric constraints, then a double helix like rAdT contains 10-fold [$(109)^{0.5}$, Table 2] less water than bulk solution.

When AE is tethered to RNA or RNA/DNA duplexes, its hydrolysis rates are inhibited to similar extents as when it is bound to the minor groove of DNA (Table 2 and ref *3*). Thus our measurements argue that when the double helix forms in solution, it excludes bulk water from its grooves. The absence of significant amounts of bulk water in the grooves of the double helix has also been observed by NMR measurements (*21*). In certain cases, such as the minor-groove spine, water can bind to the grooves of the helix. However, this water is immobilized and thus is distinguished from bulk water. Our finding that mismatches, regardless of their sequence or structure, induce rehydration of the double helix argues that the exclusion of bulk water from the helix is an intrinsic property of the double helix that is important to its stability and thus its function in aqueous environments.

ACKNOWLEDGMENT

We gratefully acknowledge the technical assistance of Cathy Nguyen.

REFERENCES

1. Nelson, N. C., Reynolds, M. A., and Arnold, L. J., Jr. (1992) in *Nonisotopic DNA Probe Techniques* (Kricka, L. J., Ed.) pp 275−310, Academic Press, San Diego, CA.
2. Mazumder, A., Majlessi, M., and Becker, M. M. (1998) *Nucleic Acids Res*. 26, 1996−2000.
3. Nelson. N. C., Hammond, P. W., Matsuda, E., and Becker, M. M. (1996) *Nucleic Acids Res. 24*, 4998−5003.
4. Kopka, M. L., and Larsen, T. A. (1992) in *Nucleic Acids Targeted Drug Design* (Propst, C. L., and Perun, T. J., Eds.) pp 303−374, Marcel Dekker Inc., New York.
5. Lown, J. W. (1993) in *Molecular Aspects of Anticancer Drug−DNA Interactions* (Neidle, S., and Waring, M. J., Eds.) Vol. 1, pp 322−355, Macmillan, London.
6. Dickson, R. S. (1995) M.S. Thesis, San Diego State University, San Diego, CA.
7. Zimmer, C., and Wahnert, U. (1986) *Prog. Biophys. Mol. Biol. 47*, 31−112.
8. Escude, C., Francois, J. C., Sun, J. S., Ott, G., Garestier, T. and Helene, C. (1993) *Nucleic Acids Res. 21*, 5547−5553.
9. Bruice, T. C., and Benkovic, S. (1966) *Bioorganic Mechanisms*, Vol. 1, W. A. Benjamin, Inc., New York.
10. Nelson, N. C., BenCheikh, A., Matsuda, E., and Becker, M. M. (1996) *Biochemistry 35*, 8429−8438.
11. Hammond, P. W., Wiese, W. A., Waldrop, A. A., Nelson, N. C., and Arnold, L. J. (1991) *J. Biolumin. Chemilumin. 6*, 35−43.
12. Becker, M. M., and Nelson, N. C. (1995) U.S. Patent 5,731,148.
13. Kennard, O. (1993) *J. Biol. Chem. 268*, 10701−10704.
14. Berman, H. M. (1994) *Curr. Opin. Struct. Biol. 4*, 345−350.
15. Xuan, J.-C., and Weber, T. (1992) *Nucleic Acids Res. 20*, 5457−5464.
16. Chuprina, V. P., Heinemann, U., Nurislamov, A. A., Zielenkiewicz, P., Dickerson, R. E., and Saenger, W. (1991) *Proc. Natl. Acad. Sci. U.S.A. 88*, 593−597.
17. Conte, M. R., Conn, G. L., Brown, T., and Lane, A. N. (1996) *Nucleic Acids Res. 24*, 3693−3699.
18. Maltseva, T. V., Agback, P., and Chattopadhyaya, J. (1993) *Nucleic Acids Res. 21*, 4246−4252.
19. Westhof, E. (1988) *Annu. Rev. Biophys. Biophys. Chem. 17*, 125−144.
20. Wahl, M. C., and Sundaralingam, M. (1995) *Curr. Opin. Struct. Biol. 5*, 282−295.
21. Maltseva, T., and Chattopadhyaya, J. (1995) *Tetrahedron 51*, 5501−5508.

BI9828066